

Experimental Determination of the $K\Sigma N$ Parity Using a Polarized Target*

B. D. DIETERLE,[†] JOHN F. ARENS,[‡] OWEN CHAMBERLAIN, P. D. GRANNIS,[§] MICHEL J. HANSROUL,^{||}
L. E. HOLLOWAY,^{**} CLAIBORNE H. JOHNSON, JR., CLAUDE SCHULTZ,^{††} HERBERT STEINER,
GILBERT SHAPIRO, AND D. WELDON^{‡‡}

Lawrence Radiation Laboratory, University of California, Berkeley, California

(Received 23 October 1967)

We have determined the $K\Sigma N$ parity using the reaction $\pi^+p \rightarrow K^+\Sigma^+$. A crystal containing polarized protons was used as the target. We have compared the counting rates for events produced from protons polarized parallel and antiparallel to \mathbf{P}_Σ , where \mathbf{P}_Σ is the polarization of Σ 's produced from unpolarized protons and has been previously measured. A higher counting rate was obtained for events for which the protons were polarized parallel to \mathbf{P}_Σ . This means that the $K\Sigma N$ parity $\Pi_{K\Sigma N} = \Pi_{\pi p} = -1$. This result depends only on the assumptions of spin $\frac{1}{2}$ for the Σ and parity conservation in the reaction. The relative probability of odd-versus-even $K\Sigma N$ parity is 21:1. Our result agrees with the usual expectations (as from SU_3) and with a previous experimental determination.

I. INTRODUCTION

THE method we have used to determine the relative intrinsic parity of the K and Σ particles ($\Pi_{K\Sigma}$) is due to Bilenky,¹ who shows that the differential cross section for production of a $K\Sigma$ final state by a pion-proton collision is of the form

$$\frac{d\sigma}{d\Omega}(\theta, \phi) = \frac{d\sigma}{d\Omega}(\theta) |{}_0[1 + \Pi T P_\Sigma(\theta)]. \quad (1)$$

Π is the product of the initial- and final-state intrinsic parities and is equal to $\Pi_{K\Sigma} \times \Pi_{\pi p}$. Note that $\Pi = -\Pi_{K\Sigma N}$. T is the component ($\mathbf{T} \cdot \hat{n}$) of proton polarization parallel to the normal of the production plane. This normal is taken to be

$$\hat{n} = \mathbf{k}_K \times \mathbf{k}_\pi / |\mathbf{k}_K \times \mathbf{k}_\pi|.$$

P_Σ and $d\sigma/d\Omega|_0$ are the polarization ($\mathbf{P}_\Sigma \cdot \hat{n}$) and differential cross section for production from an unpolarized proton target. The only assumptions necessary in the derivation of (1) are that parity is conserved and that the Σ has spin $\frac{1}{2}$.

At the pion energy and angular region of our experiment and with our definition of \hat{n} , the average Σ polarization is known to be positive, as determined from experiments with unpolarized targets.²⁻⁴

* Work done under the auspices of the U. S. Atomic Energy Commission.

[†] Present address: SLAC, Stanford University, Stanford, Calif.

[‡] Present address: Goddard Space Flight Center, Greenbelt, Md.

[§] Present address: State University of New York, Stony Brook, N. Y.

^{||} Present address: CEN-SACLAY, Essonne, France.

^{**} Present address: University of Illinois, Urbana, Ill.

^{††} Present address: Columbia University, New York, N. Y.

^{‡‡} Present address: Los Alamos Scientific Laboratory, Los Alamos, N. M.

¹ S. M. Bilenky, Nuovo Cimento **10**, 1049 (1958).

² Joseph C. Doyle, Frank S. Crawford, and Jared Anderson, Phys. Rev. **165**, 1483 (1968); Frank S. Crawford, Fernand Gard, and Gerald A. Smith, *ibid.* **128**, 368 (1962).

³ Roger O. Bangert, Angela Barbaro-Galtieri, J. Peter Berge, Joseph J. Murray, Frank T. Solmitz, M. Lynn Stevenson, and Robert D. Tripp, Phys. Rev. Letters **17**, 495 (1966).

⁴ Bruce Cork, Leroy Kerth, W. A. Wenzel, James W. Cronin, and R. L. Cool, Phys. Rev. **120**, 1000 (1960).

Complete separation of events produced from polarized protons cannot be made and the final sample of events contains "background" events produced from nucleons bound in complex nuclei in our polarized target. These bound nucleons are not significantly polarized and thus serve only to dilute the effect.

The number of events produced at any angle is the sum of background events (b) and events from free hydrogen (fh).

$$\frac{d\sigma}{d\Omega} = \frac{d\sigma}{d\Omega} \Big|_b + \frac{d\sigma}{d\Omega} \Big|_0 (1 + \Pi T P_\Sigma).$$

The production cross section for a target whose polarization is in the direction \hat{n} is

$$\frac{d\sigma}{d\Omega} \Big|_{\text{up}} = \frac{d\sigma}{d\Omega} \Big|_b + \frac{d\sigma}{d\Omega} \Big|_0 (1 + \Pi |T| P_\Sigma) = N_b + N_u.$$

For target polarization of the same magnitude, but in the direction $-\hat{n}$ we have

$$\frac{d\sigma}{d\Omega} \Big|_{\text{down}} = \frac{d\sigma}{d\Omega} \Big|_b + \frac{d\sigma}{d\Omega} \Big|_0 (1 - \Pi |T| P_\Sigma) = N_b + N_d,$$

where N_b is the cross section for K^+ events from non-hydrogen nuclei, and $N_{u,d}$ is the cross section for $K^+\Sigma^+$ events from hydrogen.

We now form a quantity ϵ , the asymmetry in counting rates for the target polarized parallel and antiparallel to the normal:

$$\begin{aligned} \epsilon &= \left(\frac{d\sigma}{d\Omega} \Big|_{\text{up}} - \frac{d\sigma}{d\Omega} \Big|_{\text{down}} \right) / \left(\frac{d\sigma}{d\Omega} \Big|_{\text{up}} + \frac{d\sigma}{d\Omega} \Big|_{\text{down}} \right) \\ &= \frac{(N_b + N_u) - (N_b + N_d)}{(N_b + N_u) + (N_b + N_d)} = \frac{N_u - N_d}{N_u + N_d + 2N_b} \\ &= \frac{N_u - N_d}{N_u + N_d} \frac{N_u + N_d}{N_u + N_d + 2N_b}. \end{aligned}$$

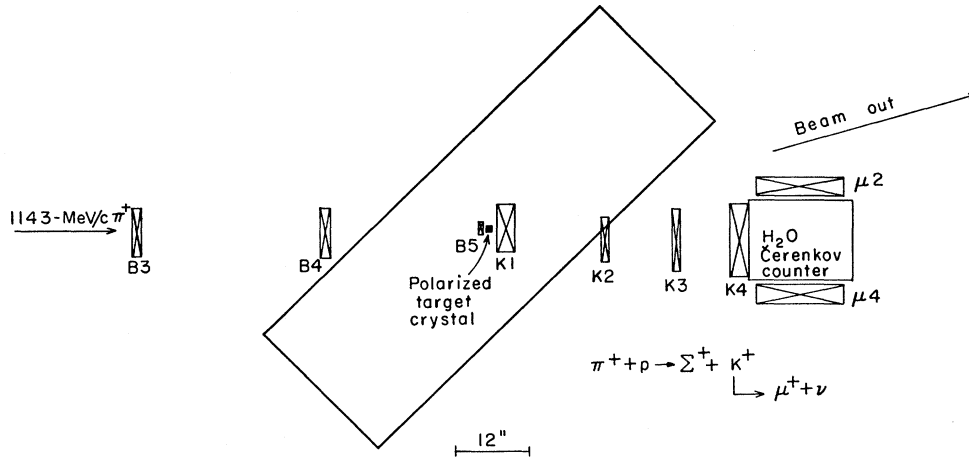


FIG. 1. Spark chamber arrangement for the detection of K^+ produced from the polarized target.

The first term is the asymmetry in counting due to the free hydrogen and the second term is a dilution of the effect due to the presence of background. We can write this as

$$\epsilon = \epsilon' f,$$

$$\epsilon' = (N_u - N_d)/(N_u + N_d) = \Pi |T| P_\Sigma,$$

$$f = (N_u + N_d)/(N_u + N_d + 2N_b) = \text{fraction of total number of events that come from free hydrogen.}$$

Thus the asymmetry in counting rate ϵ , with background included is

$$\epsilon = \Pi |T| P_\Sigma f. \quad (2)$$

$|T|$, P_Σ , and f are positive so that the sign of ϵ determines the $K\Sigma N$ parity ($\Pi_{K\Sigma N} = -\Pi$). Formula (2) assumes equal magnitudes of polarization for protons polarized in the direction \hat{n} or $-\hat{n}$. The error introduced by using formula (2) is well within the statistical accuracy of this experiment.

II. EXPERIMENTAL TECHNIQUE

A schematic diagram of the experimental apparatus can be seen in Fig. 1. A beam of 1143-MeV/c π^+ was focused on the polarized proton target polarized in a horizontal direction perpendicular to the beam. A K^+ detector placed below the beam line and the polarized target defined a vertical plane of scattering. The detector was sensitive to K^+ of momentum $370 < P_K < 600$ MeV/c. The detector was designed so that K^+ produced from free hydrogen with c.m. angles $45^\circ < \theta_{K\pi^*} < 100^\circ$ would stop near the center of the sensitive region of the detector. The sensitive region was a water Čerenkov counter C_T of inner dimensions $12 \times 12 \times 14$ in. which counted the fast decay products of the K^+ .

$$K^+ \rightarrow \mu^+ \nu, \quad \text{BR (branching ratio)} \sim 63\%,$$

$$K^+ \rightarrow \pi^+ \pi^0, \quad \text{BR} \sim 21\%.$$

Upon electronic detection of a stopping K^+ , spark chambers were fired and photographed to record the trajectories of the K^+ and its decay products as well as the incident π^+ trajectory.

The asymmetry of counting rates for $K^+\Sigma^+$ produced from free hydrogen polarized parallel or antiparallel to \hat{n} gives the $K\Sigma$ parity when Eq. (2) is used.

A. Beam

Figure 2 shows a diagram of the beam which was produced from an aluminum internal target placed in the north tangent tank straight section of the Bevatron. A bending magnet M_1 induced momentum dispersion at focus 1 where a copper slit served to select a momentum band. At focus 2 the momentum dispersion was partially cancelled. A 20-ft-long velocity spectrometer with crossed dc electric and magnetic fields caused the π^+ and protons to be separated by about 0.6 in. at focus 2. A 4-in. copper bar at f_2 intercepted the protons

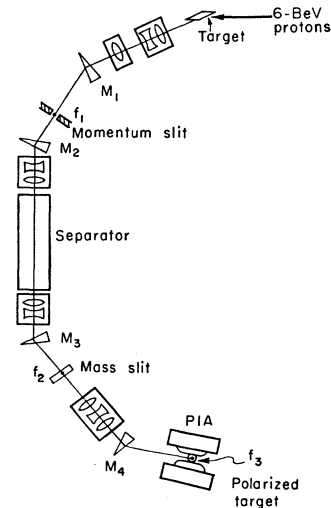


FIG. 2. Beam optics. Not shown is a beam scraper at f_1 .

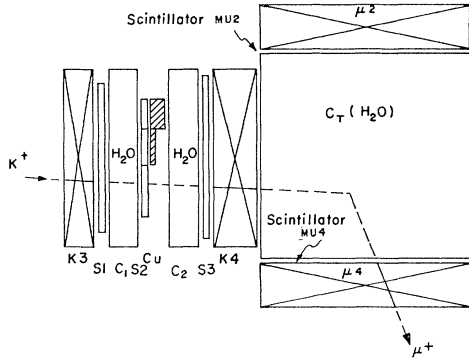


FIG. 3. K^+ range telescope. Objects labeled K and μ are spark chambers, S are scintillation counters, and C stands for Čerenkov water counter. A stopped K^+ gives the signal $[S_1(\Sigma S_2)S_3C_1C_2][C_T(\Sigma \mu)]_{\text{delayed}}$.

but not the pions. The pions were refocused downstream onto the polarized target at focus 3. Momentum dispersion was removed at f_3 by bending magnet $M4$. Accurate wire orbits were made between f_1 and f_2 and the remaining magnets were tuned empirically to maximize coincidences of $\frac{1}{4}$ -in. square counters temporarily placed at f_1 , f_2 , and f_3 . The π^+ beam momentum was obtained by correcting the wire orbit momentum by the amount of energy lost by a π^+ traversing material in the beam. The resulting beam momentum at the center of the target was 1143 MeV/c and had a spread of ± 14 MeV/c as determined by measurement of π^+ tracks in the beam spark chambers. The beam spot at f_3 was about 1.3 in. in diameter. Angular divergence in the vertical and horizontal planes was $\pm 0.6^\circ$ and $\pm 1.2^\circ$, respectively.

The maximum beam achieved was 400 000 π^+ per pulse with 2×10^{12} protons on the production target. Typical beam intensity during the experiment was 250 000 π^+ per pulse with a beam spill of 600-msec duration.

B. Polarized Target

The target consisted of four crystals of $\text{La}_2\text{Mg}_3(\text{NO}_3)_{12} \cdot 24\text{H}_2\text{O}$ with nominally 1% of the La replaced by Nd^{142} . The free hydrogen in the water of hydration was 3.2% by weight of the target, which overall had a density of 2 and weighed 19.2 g. The free hydrogen was polarized by the process of dynamic nuclear orientation which has been described in detail by other authors.⁵

Our target was operated in a field of 18.4 kG at a temperature of 1.2°K, and irradiated with about 1 W of 70-GHz microwaves. The polarization averaged 47% during the experiment. Polarization was reversed by changing the microwave frequency by 0.2%. Because

⁵ C. D. Jeffries, *Dynamic Nuclear Orientation* (Interscience Publishers, Inc., New York, 1963); G. Shapiro, *Progr. Nucl. Tech. Instr.* (North-Holland Publishing Company, Amsterdam, 1964), Vol. 1, p. 173; Claude H. Schultz, University of California Radiation Laboratory Report No. UCRL-11149, 1964 (unpublished).

the magnetic field was not changed, the geometry of the experiment was the same for both polarizations. Proton polarization was reversed every 2 h following He^4 refills of the cryostat.

C. Detection

An event of interest consisted of a single π^+ incident on the polarized target coincident in time with a K^+ emerging from the target and stopping in the K^+ telescope. π^+ were identified electronically with scintillation counters in the beam. For the beam, the coincidence logic was

$$\pi^+ = B_1 B_2 \bar{A}_{\text{hole}}$$

with B_1 a scintillation counter at focus 2 (f_2), similarly B_2 at f_3 , forming a time-of-flight coincidence which eliminated protons remaining after the separator. A_{hole} was a scintillation counter having a 1.5-in.-diam hole and placed in front of the target to veto π^+ not incident on the region of the target.

K^+ 's were identified by a K^+ telescope consisting of copper degrader, Čerenkov counters, scintillators, and spark chambers arranged as in Figs. 1 and 3. The copper degrader was a different thickness for each of the three adjacent S_2 counters. These thicknesses were chosen to stop the K^+ originating from free hydrogen near the center of the $12 \times 12 \times 14$ -in. Čerenkov counter C_T . The K^+ telescope was sensitive to elastic $K^+\Sigma^+$ events with center-of-mass (c.m.) angles $45^\circ < \theta_{K\pi^*} < 100^\circ$. K^+ outside the interval $370 \text{ MeV}/c < p_K < 610 \text{ MeV}/c$ did not stop in C_T .

For the purpose of spark-chamber triggers, a K^+ was defined to be a slow ($\beta < 0.75$) particle incident on C_T at time zero followed by a fast particle ($\beta > 0.75$) emerging from C_T in the time interval 6–50 nsec. This signified the decay of a stopped K^+ . Thus the logic used to signal electronically a possible stopped K^+ was the following:

$$K^+_{\text{stop}} = (S_1 S_2 S_3 \bar{C}_1 \bar{C}_2) \cdot (C_T \mu)_{\text{delayed } 6-50 \text{ nsec}}$$

where S_2 denotes any of the three S_2 counters and μ denotes any of the four μ counters. Spark chambers were fired by the logic pulse

$$\text{Trigger} = \pi^+ K^+_{\text{stop}} (\sim \text{DIPR}) (\sim \text{PILEUP}).$$

(“ \sim ” means “not.”) DIPR (double incident particle rejector) vetoed if two beam particles came within 450 nsec and helped protect the K^+ telescope from accidental coincidences. PILEUP integrated the beam and vetoed if the beam spark chambers had ≥ 4 tracks within their sensitive time of about 1 μsec .

Final identification of K^+ events was made by measurements of the spark-chamber tracks which were recorded on film. The intersection of the decay track of the μ spark chamber and the incident particle track in $K4$ determined the range of the stopping particle. The momentum was obtained by tracing orbits through

TABLE I. Details of counters. Counters labeled C are water-filled Čerenkov counters and the rest are scintillation counters.

Counter	Dimensions	Photomultipliers	Remarks
S_1	$10 \times 10 \times \frac{1}{2}$ in.	C70101	
S_{2A}	$10 \times 2 \times \frac{1}{2}$ in.	7264	
S_{2B}	$10 \times 2 \frac{1}{2} \times \frac{1}{2}$ in.	7264	
S_{2C}	$10 \times 3 \frac{1}{2} \times \frac{1}{2}$ in.	7264	
S_3	$11 \times 11 \times \frac{1}{2}$ in.	Two 7850's	
A_{hole}	$16 \times 3 \frac{1}{2} \times \frac{3}{4}$ in. with $1 \frac{1}{2}$ -in.-diam hole	6810A	
DIPR	5 in. diam $\times \frac{1}{4}$ in. thick	6810A	
C_1	$12 \frac{1}{2} \times 12 \frac{1}{2} \times 2 \frac{3}{8}$ in.	Six 6655A's	Wavelength shifter added
C_2	$12 \frac{1}{2} \times 12 \frac{1}{2} \times 2 \frac{3}{8}$ in.	Six 6655A's	Wavelength shifter added
C_T	$14 \frac{1}{2} \times 12 \frac{1}{2} \times 14 \frac{1}{2}$ in.	Four 58AVP's	Lined with MgO
μ_2, μ_4	$16 \frac{3}{8} \times 16 \frac{3}{8} \times \frac{3}{8}$ in.	7850	
μ_1, μ_3	$18 \frac{3}{8} \times 16 \frac{3}{8} \times \frac{3}{8}$ in.	7850	
B_1	$2 \frac{1}{2} \times 1 \frac{1}{4} \times \frac{1}{4}$ in.	7746	
B_2	$3 \frac{1}{2}$ in. diam $\times \frac{1}{4}$ in. thick	7746	

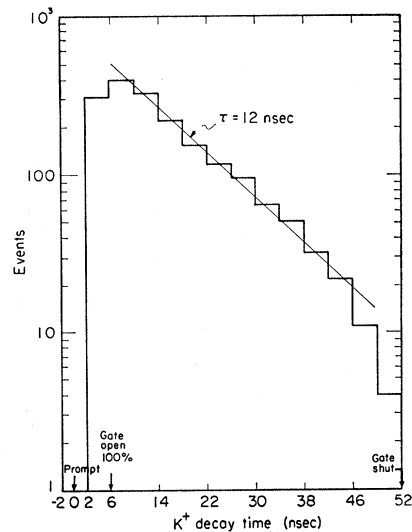
the magnetic field surrounding the target and fitting these orbits to the tracks in K_1 , K_2 , and K_3 . If the momentum was within 100 MeV/ c of the momentum obtained from K^+ range tables, the particle in the telescope was accepted as a K^+ . The π , K , and proton curves of momentum versus range differ by more than 100 MeV/ c for the band of ranges accepted by our detector. Because of the momentum resolution ($\sim 15\%$), a more stringent cutoff could have removed valid events. This criterion was sufficient to give a very pure sample of K mesons.

The electronic requirements for a trigger were sufficiently lax so that only $\sim 10\%$ of the pictures had a genuine K^+ in the K^+ telescope. This 10% had a time distribution of decay products in agreement with the 12-nsec K^+ lifetime. The time distribution in Fig. 4 shows no excess events at early time ("prompts"). The lack of "prompts" confirms that we have a clean K^+ sample.

A complete investigation into the causes of the electronic triggers which did not involve an identifiable K^+ was not undertaken. However, the same K^+ detector was used in a subsequent experiment of a similar nature⁶ in which the detector was more closely studied. Both this experiment and the later experiment agreed on the basic characteristics of the K^+ detector. Two separate classes of event triggers existed and these comprised the bulk of the events in which a K^+ could not be identified. Fifty percent of the pictures had no track in the μ chamber. These events could be explained as due to particles which hit a μ counter but missed the spark chamber. Many of these events had a small pulse in the μ counter which could have been due to Čerenkov radiation from a particle passing through its light pipe. In addition, the requirement that three gaps of a μ chamber fire meant roughly one of four particles hitting the scintillator portion of a μ counter missed the spark chamber. A rough calculation of the solid angles involved is in agreement with this interpretation for

events having no track in the μ chambers. The remainder of the false triggers were mainly prompt events. Most of these triggers were found to be due to protons. These triggers are thought to be caused by protons of $\beta \sim 0.8$ which did not fire Čerenkov veto-counters C_1 and C_2 ($\beta_{\text{thres}} = 0.75$), then fired Čerenkov counter C_T and a μ counter. Although the $(\sum \mu - C_T)$ coincidence for these events must be delayed 6 nsec from true prompts to result in a trigger, time jitter due to the physical size of the μ counter (5 nsec) and electronic effects such as discriminator time slewing would allow some coincidences. A redesign of the K^+ detector could eliminate most of the above false triggers, but would involve protecting the μ counter light pipes. Accidental triggers are negligible for our experiment.

The time distribution was obtained by measuring the time separation of the S_3 and μ scintillator pulses. All important counter pulses were displayed on a 4-beam oscilloscope and photographed each time the spark chambers fired. Periodic scans of this film were made during the run to check the electronics.

FIG. 4. Time spectrum of K^+ decays.

⁶ David M. Weldon, University of California Radiation Laboratory Report No. UCRL-17152, 1966 (unpublished). D. M. Weldon *et al.*, Phys. Rev. **167**, 1199 (1968) (accompanying paper).

TABLE II. Details of spark chamber construction. All chambers were filled with 90% Ne, 10% He.

Chamber	Dimensions	Gaps	Plate thickness	Remarks
B_1, B_2, B_3, B_4	$8 \times 8 \times 2$ in.	Eight $\frac{1}{4}$ in.	2 mil Al	Two dummy gaps
B_5	$2 \times 1\frac{1}{2} \times \frac{1}{2}$ in.	Two $\frac{1}{4}$ in.	1 mil Al	
K_1	Front face 9×3 in., back face $9 \times 1\frac{1}{2}$ in., thickness 3 in.	Twelve $\frac{1}{4}$ in.	1 mil Al	
K_2	$7 \times 7 \times 1\frac{1}{2}$ in.	Six $\frac{1}{4}$ in.	2 mil Al	Two dummy gaps
K_3	$10 \times 10 \times \frac{1}{2}$ in.	Six $\frac{1}{4}$ in.	2 mil Al	
K_4	$14 \times 12 \times 3$ in.	Eight $\frac{3}{8}$ in.	2 mil Al	
μ_2, μ_4	$14\frac{1}{2} \times 14 \times 13$ in.	Eight $\frac{3}{8}$ in.	2 mil Al	
μ_1, μ_3	$16\frac{1}{2} \times 14 \times 3$ in.	Eight $\frac{3}{8}$ in.	2 mil Al	

The π^+ trajectory was determined by four spark chambers in the beam. Two were upstream of bending magnet $M4$ and two were downstream. About 65% of the events involving K^+ had tracks in $B_1B_2B_3B_4$ of sufficient quality to reconstruct the π^+ momentum.

Tables I and II give a list of the counters and spark chambers used in the experiment.

IV. DATA ANALYSIS

Film accumulated during the experiment contained alternate blocks of data that were taken with positive target enhancement and negative enhancement. Here positive enhancement means that polarization was in the direction of the magnetic field which, for our geometry, was in the direction opposite to the normal of the scattering plane \hat{n} . Data taken with positive enhancement will often be called +data in the following text.

The data was scanned in a manner designed to equalize efficiency for the + and - data. Events selected for measurement were then measured on the SCAMP measuring-projector system at Berkeley. These events were analyzed on a 7094 computer with a program, SHERLOCK, that identified events having a genuine K^+ in the detector. Further analysis and cutoffs to remove K^+ events of low quality were done with program SUMX.

A. Scanning and Measuring

Blocks of + and - data taken near to each other in time during the experiment were scanned together on a dual projector machine. Twenty frames of + data were alternated with twenty frames of - data and the roll and frame numbers of events to be measured were recorded as encountered. Thus, each scanner selected events from equal amounts of + and - data. The alternation between the + and - data was to eliminate biases due to scanner fatigue. Projectors 1 and 2 of the dual beam projector were randomized between + and - data without the knowledge of the scanner. Because 95% of the K^+ s are produced from nonhydrogen nuclei, the number of events selected from the + data and - data should be nearly equal. This was found to be the case and serves as a check on the relative efficiency for identifying events in the + and - data.

Events were selected for measurement by the following criteria:

1. $K_2, K_3,$ and K_4 had one and only one track in them.
2. K_1 chamber had one and only one "down" track, meaning a particle that was inclined downward to the horizontal plane.
3. At least one of the four μ chambers had a track.
4. One and only one S_2 counter fired.

A track was defined to be ≥ 2 sparks in the chamber with the exception that ≥ 3 sparks were required for K_4 and the μ chambers. The K_1 chamber had alternate gaps displayed in separate views. For this chamber each split view was treated as a separate chamber and criteria (1) through (4) applied. An event was accepted if one or both split K -chamber views showed the "down" track.

Measurement of the events selected by scanning was done on the SCAMP machines at Berkeley without attempting to equalize the amounts of + and - data each scanner handled. On these machines the cross hair was adjusted manually to give the best visual fit to sparks in the chamber gaps and the $\theta, X,$ and Y film coordinates were recorded on magnetic tape.

Computer analysis with SHERLOCK reconstructed the event in three dimensions from the SCAMP film coordinates and identified events involving a K^+ .

Because good kinematic resolution was important, more stringent cutoffs were later made. The final K^+ sample satisfied the following requirements:

1. The K^+ trajectory intersected the target crystal.
2. Range momentum and the curvature momentum agreed within 100 MeV/c.
3. The K^+ track in $K4$ intersected the decay track of the μ chamber within 1.25 in., and this intersection was inside C_T .
4. K^+ tracks in chambers $K1$ through $K4$ fitted a continuous trajectory.

The total kinematic information obtained from the spark chambers and electronics was the following:

1. Identification of π^+ by time of flight.
2. Momentum \mathbf{p}_π of the π^+ .
3. Identification of K^+ .
4. Momentum \mathbf{p}_K of K^+ (best determined from observed range and checked with curvature in the magnetic field).

Information could not be obtained directly from Σ 's which decayed before reaching the $K1$ spark chamber. However, both the events of interest and the background events can result in an additional particle being present in spark chamber $K1$ via the decays:

$$\begin{aligned} \Lambda &\rightarrow p\pi^-, & \text{BR} &= 67\%, \\ \Sigma^0 &\rightarrow \Lambda\gamma & \text{BR} &= 100\%, \\ &\searrow & & \\ & p\pi^-, & \text{BR} &= 67\%, \\ \Sigma^+ &\rightarrow p\pi^0, & \text{BR} &= 50\%, \\ \Sigma^+ &\rightarrow n\pi^+, & \text{BR} &= 50\%. \end{aligned}$$

The last mode has a small solid angle for detection in $K1$. In the other decays the protons are kinematically constrained to be within about 20° of the hyperon direction. If the assumption is made that the K^+ was produced from a free proton, the Σ^+ direction can be predicted and compared to the observed proton direction. We call the angle between the Σ and proton directions $\theta_{\Sigma p}$ and define θ_{\max} as the maximum value one can have for $\theta_{\Sigma p}$ assuming the event occurred on free hydrogen.

The answers to the two questions

1. Is there an additional track in $K1$?
2. If so, is $\theta_{\Sigma p} < \theta_{\max}$?

were used to label events. All subsamples of events selected in this manner either gave no improvement in the data or contained too few events to be statistically significant. The final result did not use this selection.

For a given incident-pion momentum $K^+\Sigma^+$ events produced from free hydrogen will have a definite relation between $|\mathbf{p}_K|$ and θ_K given by the two-body kinematics. This relation can be used to eliminate a large fraction of the background events involving K^+ produced by other reactions. In the next section we describe the sources of background events and the means for reducing background.

B. Background

Because the target was composed of only 3.2% hydrogen by weight, a large number of K^+ arose from π^+ interactions in the heavier nuclei. The main background reactions were from bound neutrons (n_b) and bound protons (p_b):

$$\begin{aligned} \pi^+ n_b &\rightarrow K^+ \Lambda, \\ \pi^+ n_b &\rightarrow K^+ \Sigma^0, \\ \pi^+ p_b &\rightarrow K^+ \Sigma^+. \end{aligned}$$

In general, bound nucleons have Fermi momenta $|\mathbf{p}_F| \sim 200 \text{ MeV}/c$. Hence the K^+ produced from these nucleons will not usually have p_K and θ_K that agree with the two-body kinematics as calculated for free protons. We wish to select those events that are consistent with the kinematics of the desired reaction, $\pi^+ p \rightarrow K^+ \Sigma^+$. In order to make the selection it is

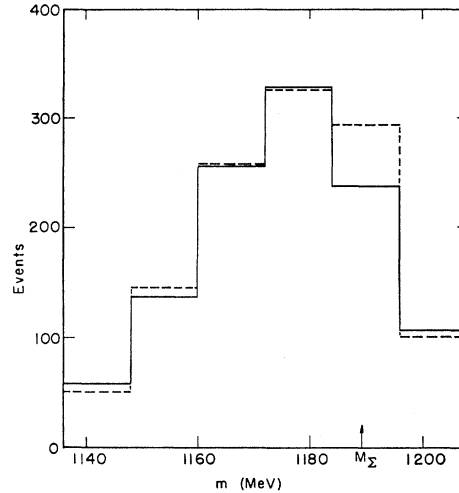


Fig. 5. Polarized target data. The dashed histogram is for negative target polarization (Σ and proton spins parallel) and the solid histogram is for positive target polarization.

necessary to calculate for each interesting event a parameter that tells how far the particular event deviates from the kinematic momentum-angle relation. There are many satisfactory ways of doing this. We have chosen a particular method, as follows. In effect we pretend that each event occurs on a free target proton and calculate the “missing mass” of a presumed unobserved hyperon. Where the observed K^+ does not fit the kinematics of the desired reaction, the so-called missing mass, called m in our formalism, deviates from the Σ mass m_Σ . For the desired events the values of m cluster around the value m_Σ . m is calculated from the relation:

$$m^2 = (E_\pi + m_p - E_K)^2 - (\mathbf{p}_\pi - \mathbf{p}_K)^2.$$

For each event the quantity m was calculated and entered in a histogram so the distribution of m values could be displayed. This “mass” distribution should show a peak centered at $m = m_\Sigma$ corresponding to events produced from free hydrogen in the crystal. Figure 5 shows the mass distribution of events produced from the polarized proton target. No peak due to hydrogen events is observed at the mass m_Σ because the peak is obscured by a large background.

To aid the separation of background, data were taken with CH_2 in place of the crystal. In the data taken with CH_2 , which effectively has four times more hydrogen per unit mass, the hydrogen peak stood sufficiently above background events to allow an estimate of its position and width. In addition, the ratio of peak to background events in CH_2 allowed us to make an estimate of this ratio for the crystal.

In principle, one might expect some background from three-body final states such as $K^+ \Lambda \pi$ and $K^+ \Sigma \pi$. However the contribution of these events is negligible. The experiment was operated at an energy lower than the threshold for producing these events in free hydrogen.

TABLE III. Summary of data.

Target	Target wt (g)	Target polarization	No. of π^+	No. of K^+ events	Events in peak region (1190 \pm 6 MeV)	Events in peak produced from protons
CH ₂	~13	0	1.4×10^9	246	88	~0.54
Crystal	19.2	+	1.0×10^{10}	1165	237	
		-	0.96×10^{10}	1090	261	
		Sum of + and -	1.96×10^{10}	2255	498	~0.22 ^a

^a Based on CH₂ data.

While three-body states might still be produced in collisions on bound nucleons, the cross section for this process is known to be small ($\lesssim 10 \mu\text{b}$ as compared to $200 \mu\text{b}$ for the desired reaction), and what few events there are must be spread thinly over a large range of the parameter m . The mass distribution for CH₂ data is shown in Fig. 6. Table III gives summaries of the data taken with CH₂ and crystal targets. Some data were taken with a target material chosen to approximate the crystal target composition without hydrogen. The distribution of these events versus m has a shape outside the peak consistent with the shape of the data taken with the crystal target and the CH₂ target. The number of events obtained from this "dummy" target is too small to make a direct determination of background in the peak region of the crystal data.

C. CH₂ Data

The events observed with the CH₂ target in place were treated in a fashion similar to events with the polarized target and a histogram of the values of m was formed, as shown in Fig. 6. The peak due to free hydrogen events stands out clearly. The background does not center at the Σ mass for several reasons. $K^+\Lambda$ events preferentially populate the lower-mass region because $m_\Lambda < m_\Sigma$. $K^+\Sigma$ events are shifted to low missing mass by the kinematics of collisions with nucleons bound in the potential well of a nucleus. The resolution of the K^+ detector also favors low-mass values to some extent.

On the basis of this histogram we chose the range

$$1184 \text{ MeV} < m < 1196 \text{ MeV}$$

as the band of m values to be used for the calculation of results (for the polarized-target data).

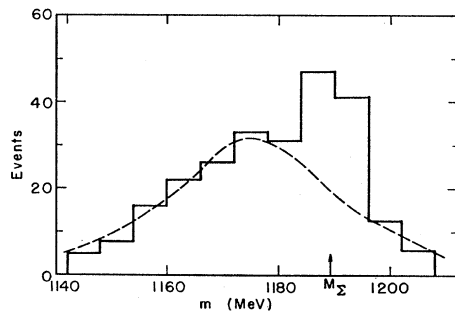


FIG. 6. CH₂ data. The dashed line is the result of a Monte Carlo calculation of K^+ production from the carbon in the target.

In the region of 1190 MeV the CH₂ data of Fig. 6 show a peak with approximately equal amounts of background and free-hydrogen events. To confirm our interpretation of the histogram we have performed a Monte Carlo calculation of the distribution to be expected from collisions on bound nucleons in carbon. A Fermi model of the nucleus was used to estimate the K^+ production angular distribution, and the detection efficiency of our apparatus was folded in. The dashed line on Fig. 6 shows the result of the calculation, normalized to the experimental data. The shape fits the data fairly well and confirms our observation of roughly equal amounts of peak and background events in the chosen band. From the Monte Carlo calculation we estimate the background to be 40 ± 7 events out of the total of 88 ± 10 events in the peak. This gives a ratio of hydrogen events to background events:

$$r_{\text{CH}_2} = \frac{\text{No. free}}{\text{No. bkgd}} = \frac{88 \pm 10}{40 \pm 7} - 1 = 1.20 \pm 0.46.$$

If we assume that heavy nuclei have reaction cross sections proportional to $A^{2/3}$, we can scale the quantity r_{CH_2} to the polarized crystal which has an average $A_{\text{crystal}} = 19$.

$$r_{\text{crystal}} = r_{\text{CH}_2} \left(\frac{\% \text{ hydrogen}}{\% \text{ heavy elements}} \right)_{\text{crystal}} \times \left(\frac{\% \text{ carbon}}{\% \text{ hydrogen}} \right)_{\text{CH}_2} \left(\frac{A_{\text{crystal}}}{A_{\text{carbon}}} \right)^{1/3}$$

$$= (1.20 \pm 0.46) \left(\frac{0.032}{0.968} \right) \left(\frac{12}{2} \right) \left(\frac{19}{12} \right)^{1/3},$$

$$r_{\text{crystal}} = 0.28 \pm 0.11$$

which yields

$$f = r_{\text{crystal}} / (1 + r_{\text{crystal}}) = 0.215 \pm 0.065.$$

This estimate depends only weakly on our use of the $A^{2/3}$ screening law. Using this value of f , the average target polarization

$$|T|_{\text{av}} = 0.47 \pm 0.10$$

and the average Σ polarization taken from bubble chamber experiments, we can now calculate the ex-

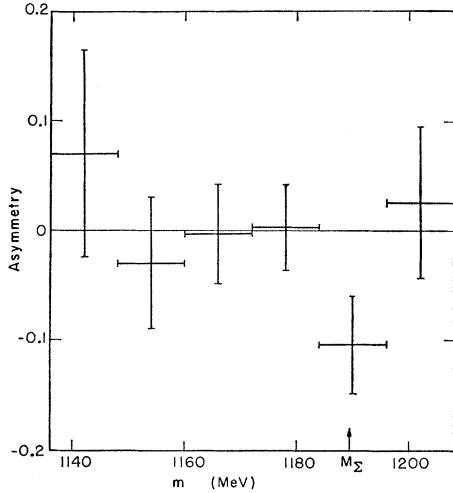


FIG. 7. Asymmetry [$\epsilon(N^+ - N^-)/(N^+ + N^-)$] in data of Fig. 5 calculated for each 12-MeV bin in m .

pected value of the raw asymmetry, ϵ_{pred} , to be observed in this experiment.

$\langle P_\Sigma \rangle$ was obtained, using the angular distribution coefficients of Doyle, Crawford, and Anderson² at 1170 MeV/ c , and averaging over the angular interval ($45^\circ < \theta_K^* < 100^\circ$) of this experiment. Although these data refer to slightly different energies, P_Σ varies slowly in this energy region, and is always positive. One finds $\langle P_\Sigma \rangle = -0.435 \pm 0.13$. Thus the expected raw asymmetry

$$\epsilon_{\text{pred}} = \langle P_\Sigma \rangle |T|f = -0.044 \pm 0.021$$

if $K\Sigma N$ parity is odd, and with the opposite sign if even.

The CH_2 data of Fig. 6 show most of the events produced from free hydrogen to be contained in the band of m values 12 MeV wide. This indicates our resolution in m for the CH_2 data of the order of 6 MeV or less. Calculation shows that the resolution for the polarized target data is of the same order of magnitude.

For each event the quantities $\pi = |\mathbf{p}_\pi|$, $K = |\mathbf{p}_K|$, $\theta = \cos^{-1}(\mathbf{p}_\pi \cdot \mathbf{p}_K / \pi K)$ have errors which contribute to the resolution width. A calculation of the resolution for a typical event gives the rms error in the parameter m .

$$\langle \delta m^2 \rangle_{\text{av}} = \langle \Delta_\theta^2 \rangle_{\text{av}} + \langle \Delta_\pi^2 \rangle_{\text{av}} + \langle \Delta_K^2 \rangle_{\text{av}} - 2 \langle \Delta_K \Delta_\pi \rangle_{\text{av}} + \text{very small cross terms,}$$

where Δ denotes the contribution of a particular measurement error.

$$\langle \delta m^2 \rangle_{\text{av}} = 14.1 + 16.4 + 5.2 - 4.3, \\ \delta m_{\text{rms}} = \pm 5.7 \text{ MeV.}$$

This can vary by about $\pm 10\%$ for other events contained in our sample.

The largest contribution to the resolution width comes from the uncertainty in the momentum measure-

ment of the incoming pion. Since our estimates rest on somewhat arbitrary assumptions in any case, we have chosen 6 MeV as our resolution for m . Any error in this width does not affect our conclusions but may change the confidence level somewhat.

V. RESULTS

Figure 5 shows the missing-mass distribution for data taken with the target protons polarized positive and negative. Data taken with negative target polarization were multiplied by 1.12 before plotting, to give equal areas outside the region 1190 ± 6 MeV. The error in this factor due to statistics alone is about 5%. If we had used beam monitors to normalize, this factor would have been 1.04. In the bin corresponding to missing mass = m_Σ there is an excess of events for the data taken with negative target polarization. Figure 7 shows a plot of the asymmetry $\epsilon = (N^+ - N^-)/(N^+ + N^-)$ for each 12-MeV bin. The asymmetry in the bin centered at 1190 MeV corresponds to greater counting rate for $K^+\Sigma^+$ production from protons polarized *parallel* to the Σ polarization direction \mathbf{P}_Σ (as found in Refs. 2 and 4). This is in agreement with odd $K\Sigma N$ relative parity. Figure 8 is a similar plot with 4-MeV-wide bins using the same data.

The asymmetry we measure is an average over the production angles $45^\circ < \theta_K^* < 100^\circ$. Its value is calculated from the data of Table III.

$$\epsilon_{\text{exp}} = \frac{237 - 1.12(261)}{237 + 1.12(261)} \\ = -0.104 \pm 0.050.$$

The error shown is statistical, including the 5% uncertainty in the normalization factor.

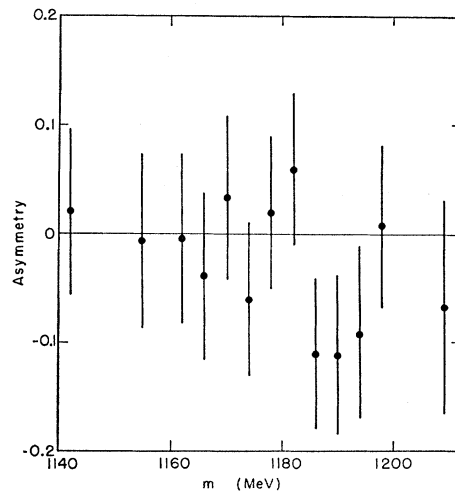


FIG. 8. Asymmetry [$\epsilon = (N^+ - N^-)/(N^+ + N^-)$] in the polarized target data plotted in 4-MeV-wide bins.

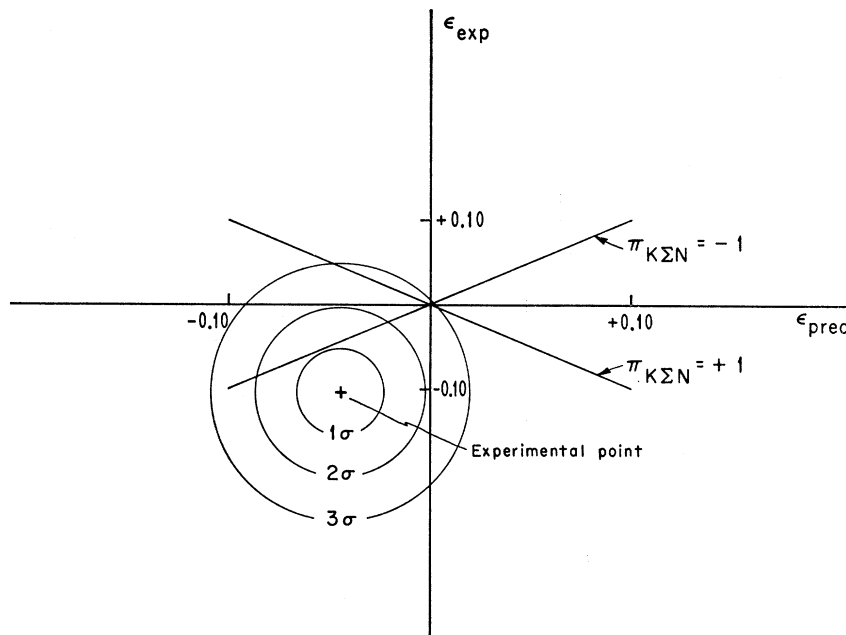


FIG. 9. Comparison of the asymmetry observed in this experiment, ϵ_{exp} , and the asymmetry predicted on the basis of polarization of Σ 's produced in unpolarized hydrogen, with the requirements of odd or even $K\Sigma N$ parity.

Figure 9 shows the comparison of ϵ_{exp} , and the ϵ_{pred} calculated above, with the theoretical possibilities allowed for the cases $\Pi_{K\Sigma N} = \pm 1$. The experimental point lies 1.1 standard deviations from the nearest point on the line corresponding to odd $K\Sigma N$ parity, and 2.7 standard deviations from the nearest point on the line corresponding to even $K\Sigma N$ parity. The ratio of probabilities for these two cases is 21:1.

This result agrees with the prediction of unitary symmetry which places the K meson in a pseudoscalar octet and the Σ hyperon in the octet of $J^{\text{parity}} = \frac{1}{2}^+$. Previous experiments to determine the $\Sigma\Lambda$ and $K\Lambda$ parity^{7,8} have been performed with the result that $\Pi_{\Sigma\Lambda} = +1$ and $\Pi_{K\Lambda} = -1$, which indirectly agrees with our result $\Pi_{K\Sigma} = \Pi_{K\Lambda}\Pi_{\Sigma\Lambda} = -1$. An earlier experimental

⁷ H. Courant, H. Filthuth, P. Franzini, R. Glasser, A. Minguzzi-Ranzi, A. Segar, W. Willis, R. Bernstein, T. Day, B. Kehoe, A. Herz, M. Sakitt, B. Sechi-Zorn, N. Seeman, and G. Snow, *Phys. Rev. Letters* **10**, 409 (1963).

⁸ M. Bock, L. Lendinara, and L. Monari, in *Proceedings of the 1962 Annual Conference on High-Energy Physics at CERN*, edited by J. Prentki (CERN, Geneva, 1962).

determination of $K\Sigma$ parity was made by Tripp *et al.*⁹ using an energy-dependent phase-shift analysis to analyze the reaction $K^-p \rightarrow Y_0^*(1520) \rightarrow \text{all channels}$. Their result, which is less free of assumptions, was also in agreement with negative $K\Sigma$ parity.

ACKNOWLEDGMENTS

The authors would like to thank the accelerator technicians for building the counters and spark chambers, and the Bevatron crew and electronic technicians for their help during the data taking. Other support groups, scanners, and summer students assisted in the various phases of the experiment and we thank them as well. Dr. Mafuzel Huq participated during part of the run, and when the experiment was in the early planning stage, Dr. Ludwig Van Rossum contributed some interesting ideas.

⁹ M. Watson, M. Ferro-Luzzi, and R. D. Tripp, *Phys. Rev.* **131**, 2248 (1963).